International Journal of Academic Multidisciplinary Research (IJAMR)
ISSN: 2643-9670
Vol. 3 Issue 11, November – 2019, Pages: 54-66

Phyto-Synthesis, Characterization and Evaluation of Antioxidant Potential of Iron Oxide Nanoparticles Using Lallemantia Royleana Seed Extract

Sadia Noor, Samina Rashid Ahmed, Maria Anwar Khan*
Department of chemistry, Lahore College for Women University, Lahore, Pakistan
*Doc.mariakhan@gmail.com

Abstract: *In the present study a simple, cost effective and eco-friendly synthesis of iron oxide Nanoparticles (IONPs) has been carried out by the reduction of iron-chloride using ascorbic acid (AA) as reducing agent and Lallemantia royleana (LR) seed extract as stabilizing agent. The Fourier transform infrared spectroscopy (FTIR) analysis revealed the polysaccharide nature of LR/extract responsible for stabilization of iron oxide Nanoparticles. Optimization of different reaction parameters (pH, temperature, amount of AA) were carried out using conventional method. The optimum conditions were found to be temperature (50°C); amount of LR/extract (10mL) and amount of AA (1.0g). The synthesized IONPs were characterized by different analytical techniques; UV-visible spectroscopy, FTIR, Atomic absorption spectroscopy (AAS), Thermal gravimetric analysis (TGA) and Atomic force microscopy (AFM). The synthesis of IONPs was confirmed successfully by UV-visible spectroscopy which measured the characteristic band of IONPs at ~370 nm. FTIR showed the interaction between IONPs and different functional groups responsible for reduction and stabilization. Unreacted amount of iron oxide nanoparticles was measured by AAS and maximum yield was found to be 83.78% by varying LR amount. The topography and surface roughness of IONPs was confirmed by AFM. The antioxidant potential of synthesized IONPs was confirmed using 2, 2- diphenyl-1-picryl-hydrazyl (DPPH), reducing power and hydroxyl radical scavenging assays which shows a concentration dependent effect on the antioxidant potential of IONPs.*

Keywords - Green synthesis; iron oxide nanoparticles; *Lallementia royleana* seed extract; antioxidant activity; fourier transform infrared spectroscopy (FTIR); thermogravimetric analysis (TGA)

1. INTRODUCTION

Nanotechnology is an emerging area of concern because of its versatile applications in the fields ranging from electronics to medicine (1). Perceptions of nanotechnology and nanostructured materials in medical applications include Analytical Tools (AT), Nano-Imaging (NI), Nanomaterial and Nano-devices (NM/ND), Modern Clinical Therapeutics (MCT) and Drug Delivery Systems (DDS), Regulatory and Toxicological Issues (RTI) (2).

Carbohydrate polymers isolated from numerous plant materials, having versatile properties, find applications in drug delivery, tissue engineering, biosensors and electronics (3). Phyto-synthesis of nanoparticles by green route is an emerging due to their availability, low cost, and eco-friendliness over the conventional chemical/physical routes. Nature represents an extraordinary reservoir of phytochemicals in the form of polyphenolic, carotenoids, terpenes, flavonoids, steroids, saponins, proteins, lipids, etc., which can play a role of reduction and capping of metallic nano-particles, thus leading to green synthesis (4). Magnetic iron oxide nanoparticles have been commonly studied for industrial and biomedical applications due to its small size and the possibility of functionalizing the surface with intended molecules (5). Moreover, iron oxides have attracted a great deal of attention among specialists because of their multivalent oxidation states, a large set of possible polymorphisms, and especially at the nano-scale, their characteristic structural changes (6).

Magnetite (Fe_3O_4) is a common magnetic iron oxide having a cubic inverse spinel structure. The compound exhibits exceptional electric and magnetic properties based upon the transfer of electrons between Fe^{2+} and Fe^{3+} in octahedral sites (7). Several chemical and physical means are used for the synthesis of iron nanoparticles. In certain methods the dispersion and uniformity of size and particle distribution were poor and provide more chances of agglomeration of nanoparticles. Likewise, physical means of synthesis are often costly because of intense energy requirement (8). Recently the synthesis of iron oxide nanoparticles using *Ficus carica* (common fig) dried fruit extract (9), zero calorie sweetener (Stevia) extract (10) and *Cynara cardunculus* leaf extract (11) are reported. Muthukumar *et al.* reported that the aqueous extract of *Amaranthus spinosus* leaf mediated iron oxide nanoparticles showed better photocatalytic and antioxidant capacity than sodium borohydride mediated nanoparticles (12).

They have huge importance in the hyperthermia cancer therapy, negative MRI contrast enhancement, drug delivery, tissue repair engineering, antibacterial, catalysis, environmental remediation, lithium-ion battery, and information storage industry (4). Treatment options against pandemic influenza strain A/H1N1 are very limited and unsatisfactory. Recently, Rishikesh Kumar *et al.,* (2018) have reported that the Antiviral activity against pandemic influenza strain A/H1N1/Eastern India/66/PR8-H1N1 shows 08 fold reductions in virus found when treated with Iron oxide nanoparticles (13). Sanjay *et al.*

investigations suggests that the antioxidant efficacy of nanoparticles/nanocomposites facilitated by graphene improves the antiradical response of iron oxide nanoparticles (14).

Due to enriched biocompatibility of iron, the use of iron oxide nanoparticles (IONPs) in nano-technological advances and biological applications has proven one of the most important transition metals oxide□based remedy (15). Among the wide amount of drug nanocarriers, magnetic iron oxide nanoparticles (IONs) can achieve high drug loading as well as targeting abilities stemming from their remarkable properties thus constitute robust nano-platforms (16). Non-functionalized BIONs with primary particle diameters of around 12 nm, as used in the process, can be produced with a simple and low-cost co-precipitation synthesis. Thus, HGMF with BIONs might pave the way for a new and greener era of downstream processing (17). Recently Zihan *et al.* suggested a way to control the *Alicyclobacillus acidoterrestris* pollution by using iron oxide nanoparticles (IONPs) modified with polydopamine were covalently immobilized with nisin (18).

Therefore, we report here the *Lallementia royleana* seeds muscilage mediated green synthesis of iron oxide NPs having exceptional high antioxidant efficacy.

2. MATERIALS AND METHODS

2.1 Chemicals

Ferric chloride ($FeCl_3.6H_2O$)**,** Ascorbic acid, NaOH, 2,2- diphenyl-1-picryl-hydrazyl (DPPH), Methanol, Sodium chloride (NaCl), Disodium hydrogen phosphate ($Na_2HPO_4.2H_2O$), Potassium chloride (KCl), Potassium dihydrogen phosphate (KH_2PO4), L- cystine, Potassium ferrocyanide (K_4 [Fe (CN) $_6$]. $3H_2O$), Trichloroacetic acid (TCA), Salicylic acid (SA), Ferrous sulphate ($FeSO_4.7H_2O$), Hydrogen peroxide (H_2O_2) were procured from Sigma Aldrich Co., USA. *Lallemantia royleana* seeds were purchased from local market.

2.2 Isolation and purification of mucilage from *LR* seeds

Weighed seeds (5.0 g) of *LR* were soaked in water (500 mL). After swelling seeds were blended in kitchen blender for one minute without breaking the seeds. The mucilage formed was then centrifuged (5000 rpm) for 15 min. The seeds were settled down and mucilage was separated as supernatant. For further purification vacuum filtration was done by using muslin cloth in order to separate remaining seeds from the supernatant. After purifying the *LR* mucilage it was stored in airtight clean bottle at 4^{o}C for further use.

2.3 Synthesis of Iron Oxide Nanoparticles

$FeCl_3.6H_2O$ solution (2.0 mM; 10 mL) was taken in round bottom flask and mixed with varying amounts (2, 4, 6, 8, 10 mL) of mucilage. pH of the reaction mixture was 3.5. The pH of mixture was adjusted at 8 by addition of NaOH (1.0 M) solution. AA (1.0 g) was added separately in each reaction mixture under vigorous stirring. Stirring was continued for about half an hour at 25^{o}C. The experiment was repeated at 60˚C. To confirm the synthesis of IONPs, UV-visible spectroscopy was used in 200-800 nm range.

2.4 Optimizations of reaction parameters

Reaction parameters (pH, temperature and amount of *LR* mucilage) were optimized to get control over the yield, size and concentration of NPs by changing the one parameter at a time and keeping rest of the parameters constant. The variables were pH (11, 12), AA (0.2-1.0 g), temperature (25 ºC & 60 ºC).

2.5 Characterization

2.5.1 UV-Vis Spectroscopy and FTIR Analysis

The formation of NPs was monitored by UV/Vis spectrophotometer (U-2800 Hitachi, Japan) to observe the characteristic λ_{SPR} of IONPs. The samples were diluted 10 times by addition of distilled water and UV-Vis spectra were recorded between 200-800 nm range. FTIR analysis of *LR* mucilage before and after synthesis was carried out by (IR Tracer-100 Shimadzu spectrometer) in the range 4000-500 cm^{-1}.

2.5.2 Atomic absorption spectroscopy and Thermo Gravimetric Analysis

The iron concentration in the reaction mixture was measured by AAS using absorption spectrometer (Shimadzu Z-5000 Hitachi, Japan) equipped with single component empty cathode lamp (6.0 mA for iron) and 10 cm of burner head and air acetylene burner for the assurance of iron. The thermal behaviour of prepared NPs were recorded under a nitrogen atmosphere at a heating rate of 10˚C/min from room temperature up to 800˚C using the (SDT Q600-TA Instruments, USA).

2.5.3 Atomic force microscopy

To study the surface morphology and distribution pattern, AFM analysis was carried out by depositing thin film of prepared NPs on copper-sheet and images were recorded by (AFM-EDX, XL30 and Philips Netherland).

2.6 *In vitro* Antioxidant Assays

2.6.1 DPPH Assay

The free radical scavenging activity was measured by using DPPH assay as reported previously (19). To perform DPPH radical assay samples were prepared by mixing (12.5, 25, 50, 100 and 200 µL/mL) of each dilution (1.0 mL) and DPPH solution (2.0 mL) to make the total volume 3.0 mL. Mixtures were shaken well and incubated in dark at 37°C for 40 min. Absorbance was measured at 517 nm by using UV-VIS spectrophotometer. Methanol was used as

positive control and DPPH solution as a negative control. Each test was performed in triplicate and percentage inhibition was measured according to following formula (1).

$$(\%) \text{ Scavenging effect} = [(A_s - A_c)/A_c] \times 100 \quad (1)$$

Where; "A_c" is absorbance of negative control and "A_s" is absorbance of test sample.

2.6.2 Reducing power assay

In this assay, various concentrations (12.5, 25, 50, 100 and 200 µL/mL) of IONPs and *LR* were separately mixed (1.0 mL) with PBS (0.2 M, pH 6.6) and potassium ferrocyanide (1.0 mL; 1%) and then incubated for 20 min. at 50 ˚C. After that TCA (1.0 mL; 10 %) was added and then centrifuged at 3000 rpm for 10 min. To supernatant (1.0 mL), DDW (1.0 mL) was added followed by of $FeCl_3$ (0.5 mL; 0.01 %) and the absorbance was measured at 700 nm against PBS as blank. AA was used as positive control in this test. The percentage inhibition was determined using the equation:

$$\% \text{ inhibition} = (A_s - A_{nc}) / (A_{pc} - A_{nc}) \times 10 \quad (2)$$

Where; "A_s" is the absorbance of test sample; "A_{nc}" is absorbance of negative control and "A_{pc}" is absorbance of positive control.

2.6.3 Hyroxyl radical scavenging assay

To different concentrations of IONPs (12.5, 25, 50, 100 and 200 µL/mL) and *LR* extract, salicylic acid (9.0 mM; 1.0 mL), $FeSO_4.7H_2O$ (9.0 mM; 1.0 mL) and H_2O_2 (1.0 mL) were added. The reaction mixture was incubated at 37 ˚C for 60 minutes. After incubation the absorbance was measured at 510 nm using a UV-visible spectrophotometer. Negative control was prepared without samples, whereas AA was taken as positive control. The percentage of hydroxyl radical scavenging activity for test samples was determined using (3)

$$\% \text{ inhibition} = [(A_0 - A_t)/A_0] \times 100 \quad (3)$$

Where "A_0" is the absorbance of the control, and "A_t" is the absorbance of test/standard.

3. RESULTS AND DISCUSSIONS

3.1 Isolation of mucilage from *LR* seeds

Lallemantia royleana (Benth.) is an essential folk medicine which is utilized in number of illnesses. phyto-chemical investigation of methanolic concentrates of *L. royleana* seeds demonstrated that the seeds extract contains Alkaloids, Anthraquinones, Flavonoids, Glycosides, Pholobtannins, Tannins and Terpenoids. The results of GC-MS examination demonstrated that no less than 21 mixes are available in methanolic concentrate of *L. royleana* (20).

3.2 Synthesis of IONPs

In the present work IONPs have been successfully synthesized from a mucilage isolated from *LR seeds* as stabilizing agent and AA as reducing agent. The color of the solution rapidly changed from yellow to dark brown by addition of $FeCl_3$ (2mM) to the acidic solution of the *LR* extract and AA, indicating the reduction of $Fe^{3+}$to Fe^{2+} as shown in Fig.1. The mechanism of this reaction involved the formation of ferric hydroxide by the hydrolysis of $FeCl_3$ in alkaline media followed by the reduction of ferric hydroxide to ferric oxide- NPs. The reaction may further facilitate by the presence of biomolecules or combination of chemically complex biomolecules such as amino acids, enzymes, proteins, vitamins, polysaccharides and organic acids such as citrates which act as reducing as well as capping agents (21). Due to high reduction potential of iron the reduction of Fe^{+3} to Fe^0 is not possible by using these weak reducing agents. AA is mild reducing agent. So in the present study AA assisted the mucilage components to synthesize the IONPs by reduction of Fe^{+3} to Fe^{+2}. The reduction time was reduced from hours to 15 min in the presence of mucilage.

Polysaccharides enriched with hydroxyl groups have been reported to interact with iron oxide via hydrogen bonding Small molecule ligands such as citric acid and mannose have been exploited as a coating material for IONPs, which provides stability to the NPs in solution and is also helpful for cellular uptake (22).

Fig. 1. *Change in colour of $FeCl_3$ from light-brown to dark-brown by addition of seed mucilage and ascorbic acid, confirmed the reduction of Fe^{+3} ions to Fe^{+2}.*

3.3 Optimization of reaction parameters

Reaction parameters such as temperature, pH, amount of mucilage and AA played critical role in synthesis of NPs. UV-spectroscopy was used to optimize all reaction parameters over synthesis of particles. UV spectra of NPs is highly sensitive to the size, shape and concentration of NPs. IONPs can absorb and scatter light in the range (250-400nm) with good efficiency because conduction-electrons of nano-metals undergo collective oscillation when light interacts. By proper use of UV spectroscopy, the control over reaction parameters can be achieved to during synthesis of NPs. So, optimization of reaction parameters was achieved conventionally by varying one parameter and keeping rest of the parameters constant and measuring their UV-VIS spectra.

3.4 Optimization of temperature and amount of AA

To optimize the reaction parameters a series of experiments were performed by varying the amount of AA (0.2 g-1.0 g), pH (11, 12) and temperature (25 ^{o}C & 60 ^{o}C) to the fix amount of $FeCl_3$ solution (2.0 mM; 10 mL). The results obtained indicated that by increasing the amount of AA the λ_{max} shifted slightly toward shorter wavelength (376-370 nm) whereas absorbance increased at both reacting temperatures 25˚C and 60˚C. By varying the pH, the maximum absorbance was observed at pH 8. It was also observed that reaction rate was faster at high temperature, low pH, large amount of AA and amount of mucilage. In the presence of mucilage, the reaction was rapid and in its absence the reaction rate was too slow and colour change was observed after two weeks. So, the role of mucilage can be understood, it not only acting as stabilizing agent but also assist in reduction of precursor ions. The spectral variations with varying amount of AA, temperature and pH are shown in Fig. 2 & 3.

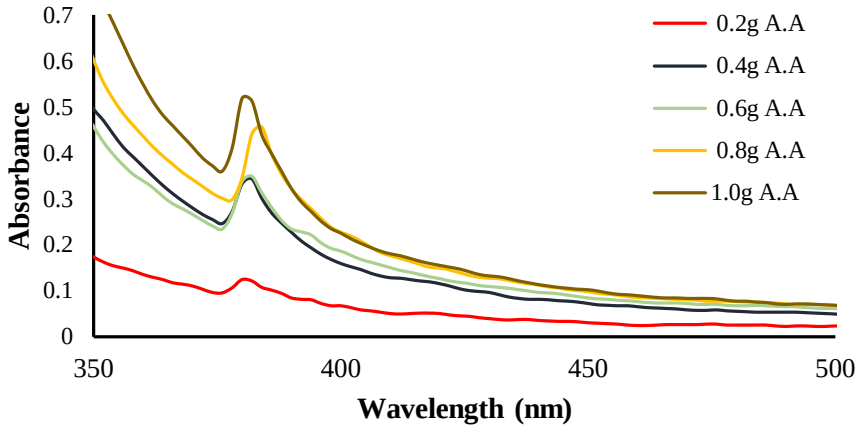

(A)

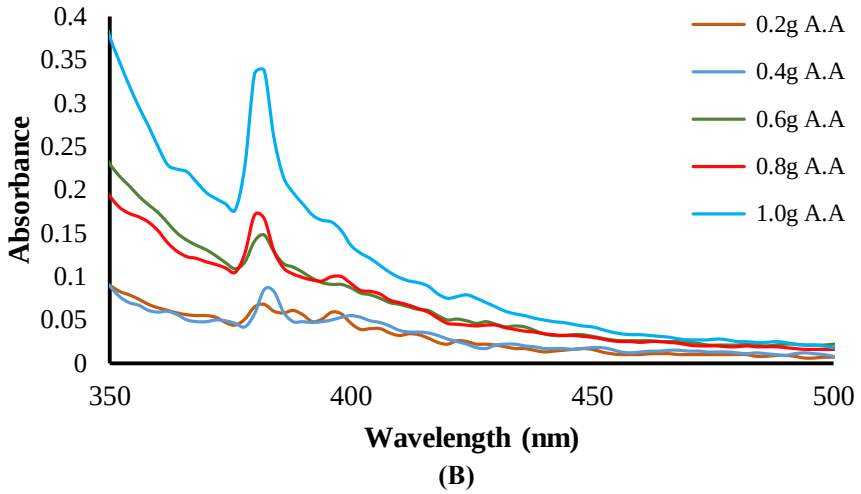

(B)

Fig. 2. *Variation in surface plasmon resonance (SPR) spectra by the amount of ascorbic acid at (A) 60 ˚C (B) 25˚C and pH 12*

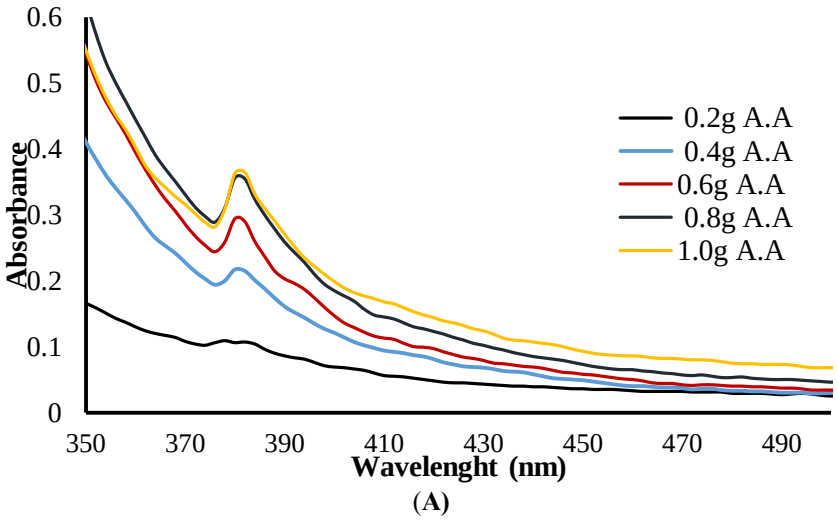

(A)

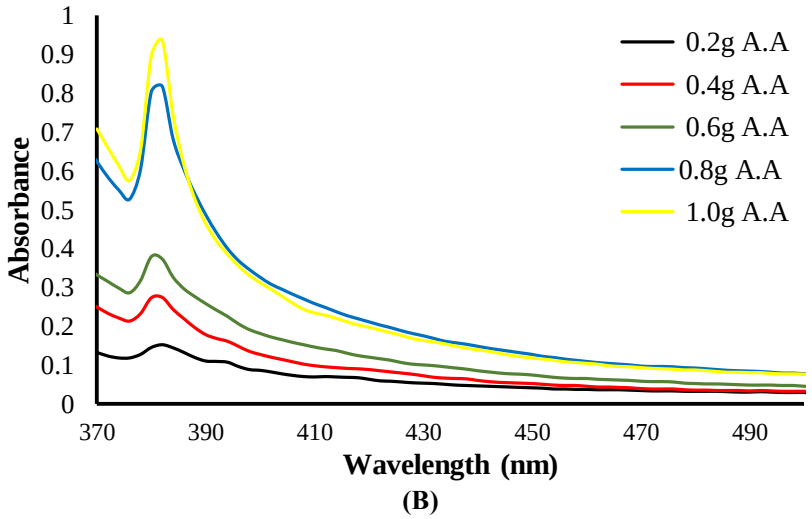

(B)

Fig. 3. *Variation in surface plasmon resonance (SPR) spectra by the amount of ascorbic acid at (A) 60 ˚C (B) 25˚C and pH 11*

3.5 Characterization of IONPs

3.5.1 UV-Vis spectroscopic analysis and FTIR spectroscopy

To verify the presence of IONPs UV-visible spectrometer was used within the range of (200-800) wavelength. Two peaks were observed in the spectra of synthesized IONPs, at ~370 nm and ~ 340 nm indicating the presence of IONPs and $FeCl_3$. The maximum value for λ_{SPR} was 376 nm, that was recorded at 50˚C which is a characteristic of spherical shaped IONPs. By increasing the amount of mucilage maximum absorbance was observed as shown in Fig. 4. Behera, S. S., reported that the IONPs showed a higher peak at 370nm as a valid standard reference by UV-Visible spectroscopy (23).

The FTIR analysis showed a characteristic peak of O-H (~3387.0 cm-^{1}), N-H (~3284.7736), C-H group (~ 2920.227424 cm^{-1}) and C=C group (1600-1680 cm$^{-1)}$ in mucilage as shown in Fig. 5. The broad spectral band at approximately 3400cm^{-1} and two intense bands at 2919 cm^{-1} and 2850 cm^{-1} were attributed to the asymmetric and symmetric stretching of C-H vibrations of the methylene group of aliphatic compounds present in muscilage disappeared after the formation of IONPs. The bands in the range of (590-571 cm^{-1}) and (455-412 cm^{-1}) are ascribed to the structural vibrations which confirm the presence of metal oxide stretching band.

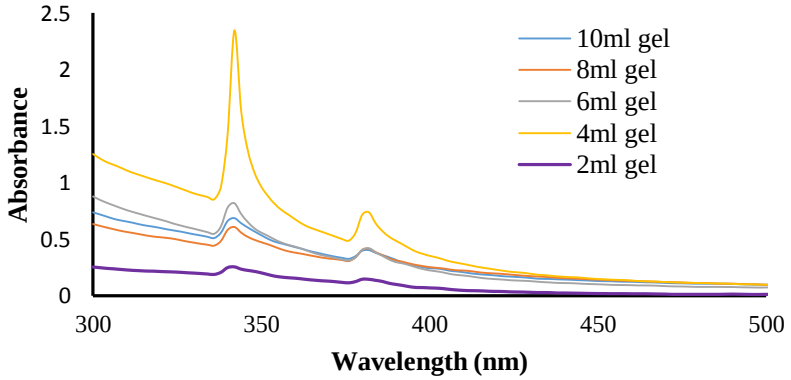

Fig. 4. *Synthesis of iron oxide nanoparticles (IONPs) by varying amount of mucilage at 50˚C*

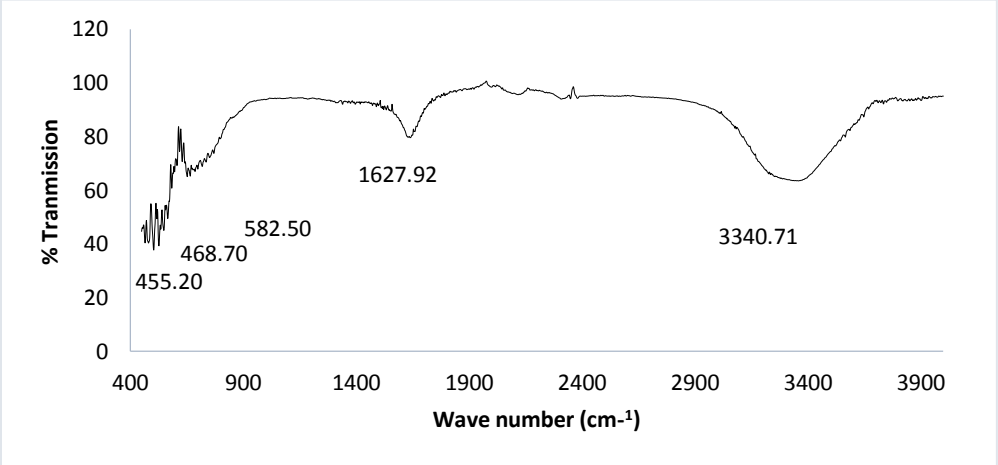

(A)

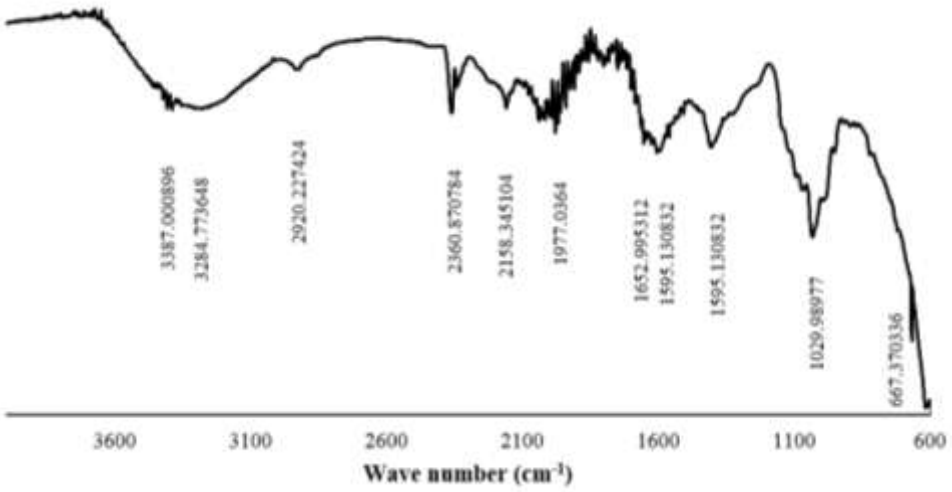

(B)

Fig. 5. *Fourier-transform infrared spectroscopy (FTIR) spectrum of A) Iron oxide nanoparticles (IONPs) B) Lallemantia royleana (LR) mucilage with IONPs*

3.5.2 Atomic absorption spectroscopy and Thermal analysis

AAS was used to analyze the concentration of Fe^{+2} ions in reaction mixture after synthesis. The effect of *LR* mucilage concentration was studied using this technique. The result demonstrated that Fe-ions concentration significantly reduce due to the conversion of Fe^{+3} to Fe^{+2}. The graph was plotted between concentrations (ppm) of IONPs and absorbance a straight line was obtained as shown in Fig. 6 & 7. The straight-line equation was used to calculate the concentration of IONPs Table 1.

The thermal behavior of IONPs were characterized by TGA analysis at a range of 20-800^{o}C. The result of TGA analysis showed a weight loss most probably due to the loss of gust water and decomposition of organic functional groups, as temperature increases from room temperature to 200^{o}C. The result showed a three weight loss stages first observed at 91.74^{o}C then 200^{o}C. At the third stage (200-700^{o}C) the weight loss changes were minimized, and little weight loss was observed. Similarly, the TGA analysis of pure *LR* mucilage was also carried out in a temperature range of 20-800^{o}C. Three sharp break points as shown in Fig. 13 first at 132.83 then at 247.91and finally at 330^{o}C. The weight loss rate become negligible at (330 ^{o}C-700^{o}C) as shown in Fig. 8.

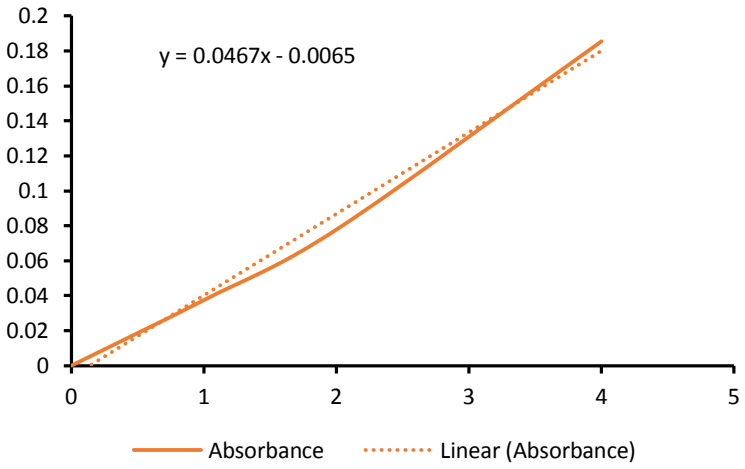

Fig. 6. *Absorbance variation with concentration of LR/extract [parts per million] (PPM)*

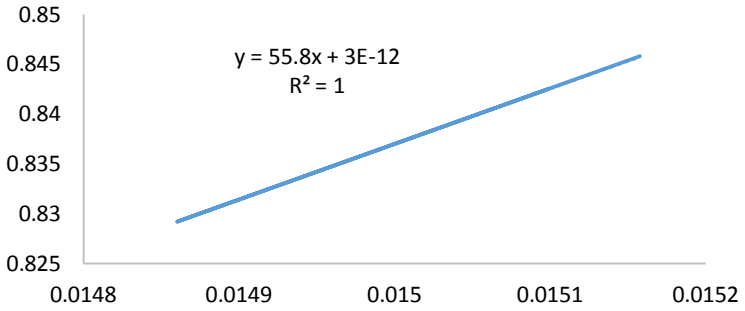

Fig. 7. *Absorbance variation with concentration of unreactive IONPs (moles/dm^3)*

Table 1: Concentration and % yields of iron oxide nanoparticles (IONPs) determined by varying *Lllemantia royleana (LR) mucilage*

Amount of mucilage (mL)	*$FeCl_3$ (mL)*	*Amount Of A.A (g)*	*(Abs)*	*Conc. Of Fe^{+3} ions (unreacted) (x) Ppm*	*Conc. of IONPs (ppm) (reacted)*	*Conc. of IONPs (mol/dm^3)*	*Yield (%)*
		60 °C					
10	10	0.15	0.8425	18.17987152	91.82012	0.0016455	83.529036
8	10	0.15	0.8385	18.09421842	91.905781	0.0016470	83.606955
6	10	0.15	0.8336	17.98929336	92.010706	0.0016489	83.702405
4	10	0.15	0.8292	17.89507495	92.104925	0.0016506	83.788116
2	10	0.15	0.8458	18.25053533	91.749464	0.0016442	83.464753

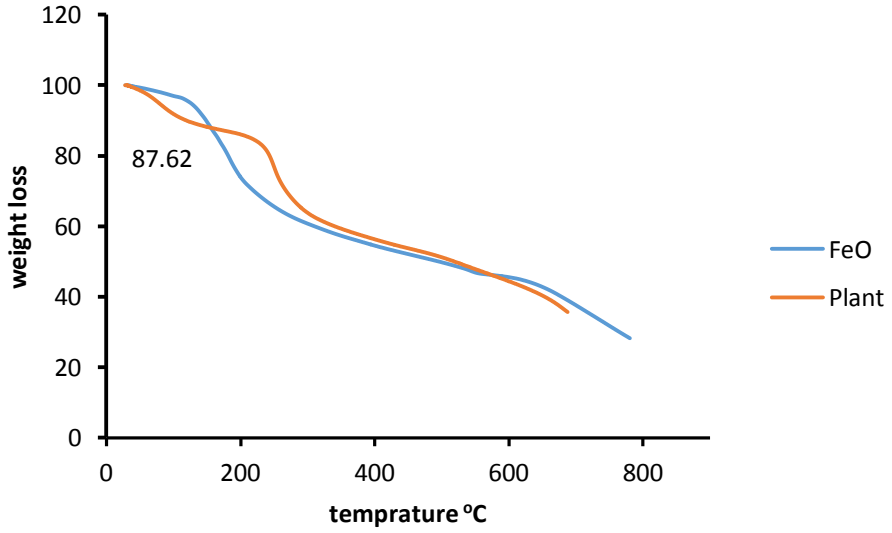

Fig. 8. *Thermogravimetric analysis (TGA) analysis of iron oxide nanoparticles (IONPs) and pure Lallemantia royleana (LR)/ extract*

3.5.3 Atomic Force Microscopy

For the AFM imaging of IONP samples, sample were deposited onto freshly cleaved copper sheets. Surface morphology of IONPs are depicted in the AFM image Fig. 9. The roughness of the surface is due to dispersion of the NPs in polymeric matrix.

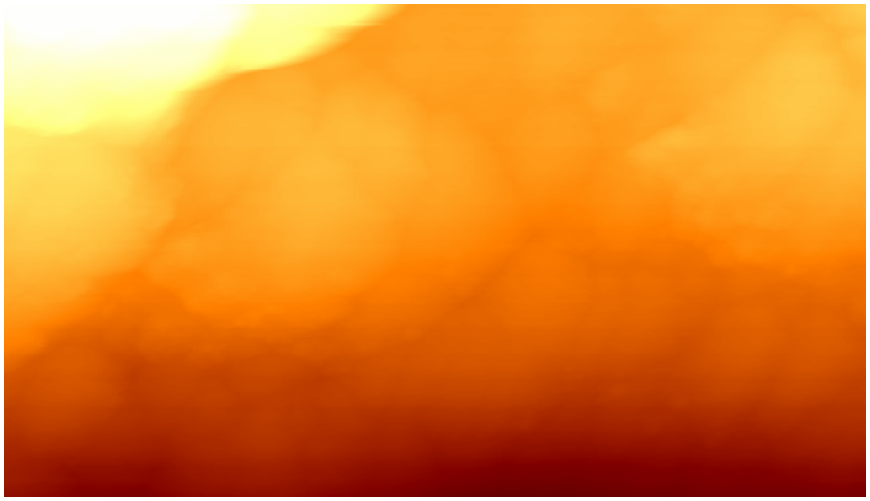

Fig. 9. *Atomic force microscopy (AFM) image of iron oxide nanoparticles (IONPs)*

3.6 Assessment of antioxidant activity of IONPs

3.6.1 DPPH assay

In present experiments, the total anti-oxidation effect of synthesized IONPs and extracted *LR* mucilage using (200, 100, 50, 25, 12.5ul/ml) dilutions was determined. Absorbance recorded for DPPH was (2.149). AA was used as a positive control. The color of the DPPH solution in the presence of the IONPs changes gradually from deep violet to pale yellow as shown in Fig. 10 which gives the visual monitoring of the antioxidant activity of the NPs. From the UV–Vis absorption spectra graph shown in Fig. 11, it can be inferred that with the increase in concentration of the NPs, the anti-oxidant potential was also increased. (%) Scavenging effect was calculated using formula:

(%) Scavenging effect = $[(A_s)/A_c] \times 100$ (4)

A_s= absorbance of sample A_c=absorbance of control (DPPH)

Now using formula percentage activity has been calculated.

The antioxidant activity of reducing sugars is mainly due to their redox properties, which can play an important role in absorbing and neutralizing free radicals, quenching singlet and triplet oxygen, or decomposing peroxides (24).

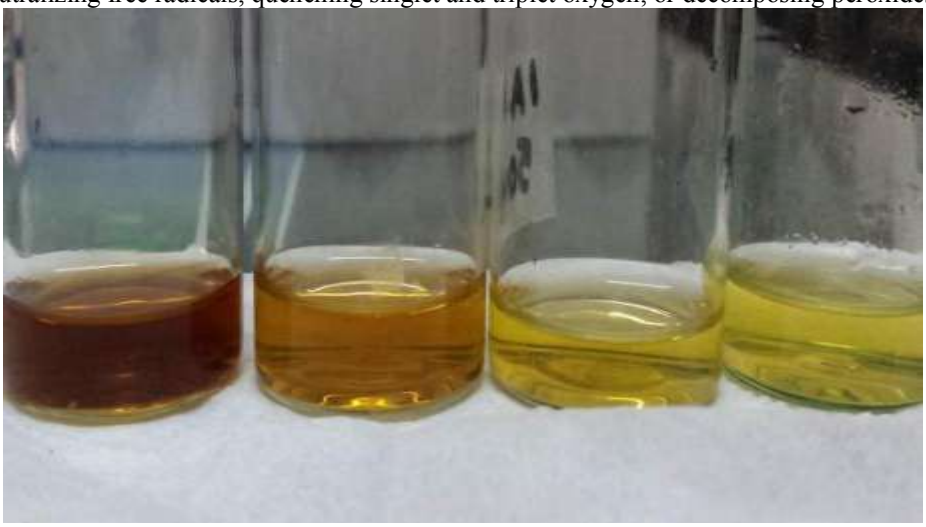

Fig. 10. *2,2-diphenyl-1-picrylhydrazyl (DPPH) scavenging (%) increases with increase in amount of IONPs and time*

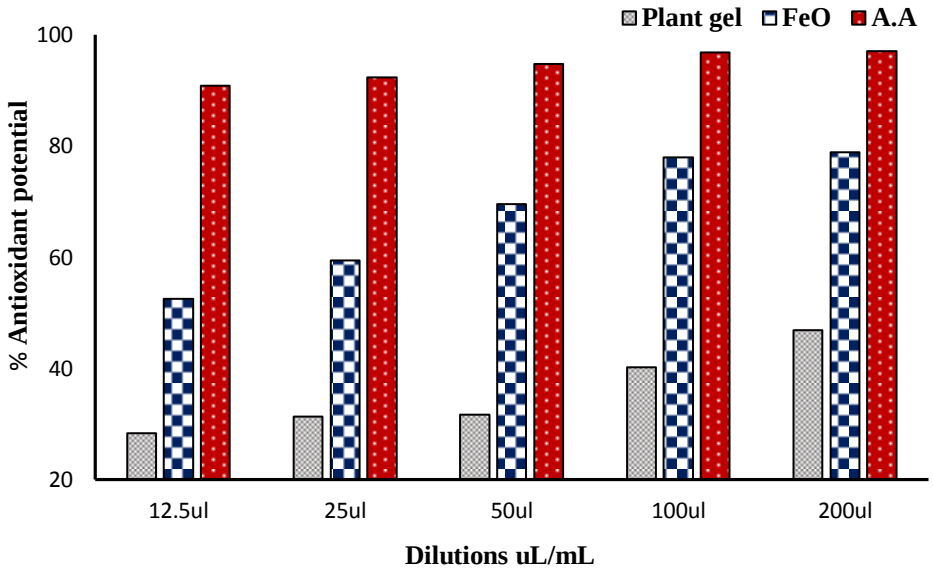

Fig. 11. *Antioxidant activity of iron oxide nanoparticles (IONPs) against 2,2-diphenyl-1-picrylhydrazyl (DPPH)*

The DPPH scavenging activities for the iron oxide particles, S_1 (0 min), S_2 (15 min) and S_3 (30 min) were found to be in the order: $A_{S3}>A_{S2}>A_{S1}$. Where A_{S1}, A_{S2} and A_{S3} are the DPPH scavenging activities for the sample S_1, S_2 and S_3, respectively. The iron oxide particles quenched the DPPH free radicals in a dose-dependent manner, as the concentration of iron oxide particle increases the DPPH quenching activity also increased as shown in Fig. 12.

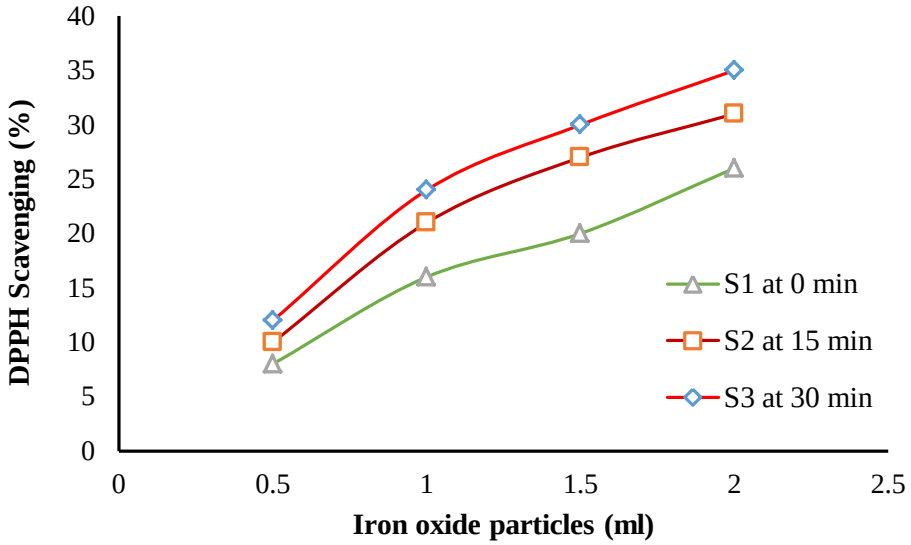

Fig. 12. *DPPH scavenging (%) increases with increase in amount of IONPs and time*

3.6.2 Hydroxyl radical scavenging assay

Hydroxyl radical scavenging effect of IONPs and *LR mucilage* was investigated through this assay and these results were shown as relative activity against the standard (AA). The results showed that IONPs were equally potent in scavenging the hydroxyl radicals. Formulated nanoparticles possess unique morphology, large surface area which can easily accept electrons from (•OH) radical. The dose depended (•OH) radical scavenging ability of IONPs was mainly due to the presence of antioxidant moieties i.e. reducing sugars from the *LR* mucilage. Fig. 13 displays the dose-depended ferric ion reduction ability of IONPs.

3.6.3 Reducing power assay

Scavenging activity of *LR* mucilage and IONPs which is shown in Fig. 14, concluded that the IONPs have less scavenging activity as compared to the *LR mucilage* because the pure plant extract is a rich source of reducing sugars which shows maximum activity. The dilution containing maximum concentration of IONPs and *LR mucilage* shows maximum scavenging potential. Different dilutions of AA shows maximum scavenging potential. AA has been shown to be an excellent antioxidant under both in vitro and in vivo study conditions. However, in the presence of catalytic metal ions, vitamin C can also function as a pro-oxidant. Specifically, vitamin C has been found to be capable of converting Fe^{3+} into Fe^{2+}, which subsequently reacts with oxygen or hydrogen peroxide to form superoxide and hydroxyl radicals that can subsequently damage biomolecules (25).

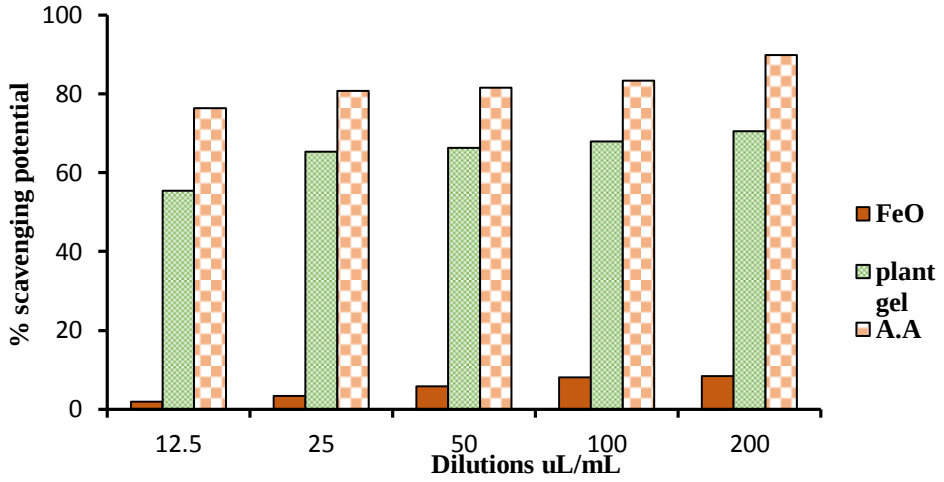

Fig. 13. *Hydroxyl radical scavenging assay of LR mucilage and IONPs*

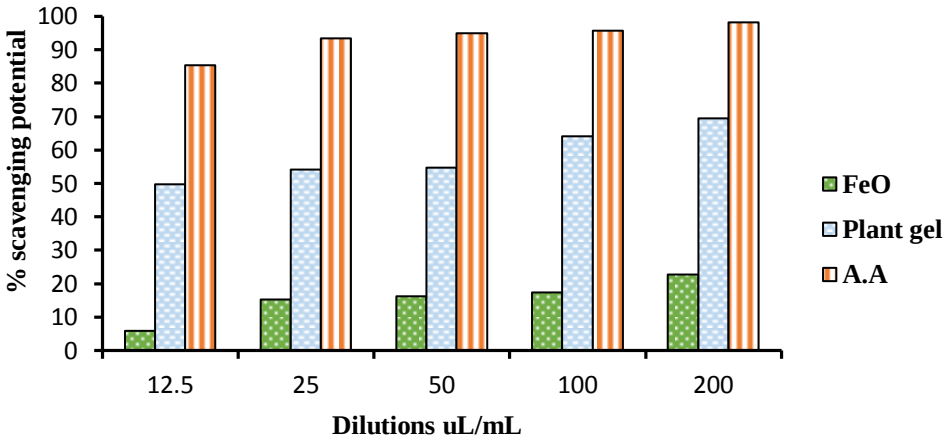

Fig. 14. *Reducing power of iron oxide nanoparticles (IONPs)*

CONCLUSION

This study presents eco-friendly, economical, simple and fast method based on green chemistry approach for the synthesis of IONPs by the reduction of iron-chloride using ascorbic acid as reducing agent and *LR* seed extract as stabilizing agent. Our results indicate impressive antioxidant properties of the biosynthesized IONPs. The antioxidant potential of synthesized IONPs has been confirmed using DPPH, reducing power and hydroxyl radical scavenging assays. The significant antioxidant activity suggests that the IONPs could be a potential candidate for various biomedical applications.

SUGGETIONS

However, to harvest the true benefits of these biologically synthesized nanomaterials, further *in vitro* and *in vivo* studies are suggested by involving animal models that can help in fabrication of iron oxide nanomaterials with highest degree of biocompatibility.

5. ACKNOWLEDGEMENT

The authors are thankful to the Chemistry Department of Lahore College for Women University.

CONFLICT OF INTEREST: Nil

6. REFERENCES

[1] Amin, M., Iram, F., Iqbal, M. S., Saeed, M. Z., Raza, M., & Alam, S. (2013). Arabinoxylan-mediated synthesis of gold and silver nanoparticles having exceptional high stability, Carb. Poly., vol. 92(2), pp. 1896-900.

[2] Nochehdehi, A. R., Thomas, S., Sadri, M., Afghahi, S. S., & Hadavi, S. M. (2017). Iron oxide biomagnetic nanoparticles (IO-BMNPs); synthesis, characterization and biomedical application–a review, J. Nanomed. Nanotech., vol. 8(1), pp. 1-9.

[3] Iram, F., Iqbal, M. S., Athar, M. M., Saeed, M. Z., Yasmeen, A., & Ahmad, R. (2014). Glucoxylan-mediated green synthesis of gold and silver nanoparticles and their phyto-toxicity study, Carb. Poly., vol. 104, pp. 29-33.

[4] Kumar, B., Smita, K., Cumbal, L., Debut, A., Galeas, S., & Guerrero, V. H. (2016). Phytosynthesis and photocatalytic activity of magnetite (Fe3O4) nanoparticles using the Andean blackberry leaf, Mat. Chem. Phy., vol. 179, pp. 310-315.

[5] Rost, N. C., Broca, F. M., Gonçalves, G. C., Cândido, M. A., Castilho, M. L., & Raniero, L. J. (2019). Synthesis of Iron Oxide Nanoparticles Optimized by Design of Experiments, Braz. J. Phy., vol. 49(1), pp. 22-27.

[6] Balamurugan, M., Saravanan, S., & Soga, T. (2014). Synthesis of iron oxide nanoparticles by using Eucalyptus globulus plant extract, J. Sur. Sci. Nanotech., vol. 12, pp. 363-267.

[7] Mahdavi, M., Namvar, F., Ahmad, M., & Mohamad, R. (2013). Green biosynthesis and characterization of magnetic iron oxide (Fe3O4) nanoparticles using seaweed (Sargassum muticum) aqueous extract, Molecules, vol. 18(5), pp. 5954-5964.

[8] Khalil, A. T., Ovais, M., Ullah, I., Ali, M., Shinwari, Z. K., & Maaza, M. (2017). Biosynthesis of iron oxide (Fe2O3) nanoparticles via aqueous extracts of Sageretia thea (Osbeck.) and their pharmacognostic properties, Green Chem. Lett. Rev., vol. 10(4), pp. 186-201.

[9] Demirezen, D. A., Yıldız, Y. Ş., Yılmaz, Ş., & Yılmaz, D. D. (2019). Green synthesis and characterization of iron oxide nanoparticles using Ficus carica (common fig) dried fruit extract, J. biosci. Bioeng., vol. 127(2), pp. 241-245.

[10] Khatami, M., Alijani, H. Q., Fakheri, B., Mobasseri, M. M., Heydarpour, M., Farahani, Z. K., & Khan, A. U. (2019). Super-paramagnetic iron oxide nanoparticles (SPIONs): Greener synthesis using Stevia plant and evaluation of its antioxidant properties, J. Cleaner Pro., vol. 208, pp. 1171-1177.

[11] de Jesús, Ruíz-Baltazar, Á., Reyes-López, S. Y., de Lourdes, Mondragón-Sánchez, M., Robles-Cortés, & AI., Pérez, R. (2019). Eco-friendly synthesis of Fe3O4 nanoparticles: Evaluation of their catalytic activity in methylene blue degradation by kinetic adsorption models, Res. Phy., vol. 12, pp. 989-995.

[12] Muthukumar, H., & Matheswaran, M. (2015). Amaranthus spinosus leaf extract mediated FeO nanoparticles: physicochemical traits, photocatalytic and antioxidant activity, A. C. S. Sus. Chem. Eng., vol. 3(12), pp. 3149-3156.

[13] Kumar, R., Nayak, M., Sahoo, G. C., Pandey, K., Sarkar, M. C., Ansari, Y., Das, V. N., Topno, R. K., Madhukar, & M., Das, P. (2019). Iron oxide nanoparticles based antiviral activity of H1N1 influenza A virus. J. Infect. Chemother., vol. 25, pp. 325-329.

[14] Hastak, V., Bandi, S., Kashyap, S., Singh, S., Luqman, S., Lodhe, M., Peshwe, D. R., & Srivastav, A. K. (2018). Antioxidant efficacy of chitosan/graphene functionalized superparamagnetic iron oxide nanoparticles, J. Mat. Sci: Mat. Med., vol. 29(10), pp. 154.

[15] Saqib, S., Hussain, Munis, M. F., Zaman, W., Ullah, F., Shah, S. N., Ayaz, A., Farooq, M., & Bahadur, S. (2018). Synthesis, characterization and use of iron oxide nano particles for antibacterial activity, Micro. Res. Tech., vol. 84, pp. 415-420.

[16] Vangijzegem, T., Stanicki, D., & Laurent, S. (2019). Magnetic iron oxide nanoparticles for drug delivery: applications and characteristics, Expert Op. Drug Deliv., vol. 16(1), pp. 69-78.

[17] Schwaminger, S. P., Fraga-García, P., Blank-Shim, S. A., Straub, T., Haslbeck, M., Muraca, F., Dawson, K. A., & Berensmeier, S. (2019). Magnetic One-Step Purification of His-Tagged Protein by Bare Iron Oxide Nanoparticles. A. C. S. Omega, vol. 4(2), pp. 3790-3799.

[18] Song, Z., Wu, H., Niu, C., Wei, J., Zhang, Y., & Yu`e, T. (2019). Application of iron oxide nanoparticles@ polydopamine-nisin composites to the inactivation of Alicyclobacillus acidoterrestris in apple juice, Food Chem., vol. 287, pp. 68-75.

[19] Sathishkumar, G., Jha, P. K., Vignesh, V., Rajkuberan, C., Jeyaraj, M., Selvakumar, M., Jha, R., & Sivaramakrishnan, S. (2016). Cannonball fruit (Couroupita guianensis, Aubl.) extract mediated synthesis of gold nanoparticles and evaluation of its antioxidant activity, J. Mol. Liquids, vol. 215, pp. 229-236.

[20] Fatima, J., Mansoor, S., Ali, S., M., Rehman, M., & Mustafa, H. (2016). Phyto-Chemical Analysis, In-Vitro Antioxidant Potential and GC-MS of *Lallemantia royleana* Seeds, Inter. J. Sci. Res. Pub., vol. 6(2), pp. 407-411.

[21] Saif, S., Tahir, A., & Chen, Y. (2016). Green synthesis of iron nanoparticles and their environmental applications and implications, Nanomaterials, vol. 6(11), pp. 209.

[22] Reza, K. M., Kurny, A., & Gulshan, F. (2016). Photocatalytic degradation of methylene blue by magnetite+ H_2O_2+ UV Process, Inter. J. Envir. Sci. Dev., vol. 7(5), pp. 325.

[23] Behera, S. S., Patra, J. K., Pramanik, K., Panda, N., & Thatoi, H. (2012). Characterization and evaluation of antibacterial activities of chemically synthesized iron oxide nanoparticles, W. J. of Nano Sci. Eng., vol. 2(04), pp. 196.

[24] Prakash, M. J., & Kalyanasundharam, S. (2015). Biosynthesis, characterisation, free radical scavenging activity and anti-bacterial effect of plant-mediated zinc oxide nanoparticles using *Pithecellobium dulce* and *Lagenaria siceraria* Leaf Extract, World Sci. News, vol. (12), pp. 100-117.

[25] Kasote, D. M., Katyare, S. S., Hegde, M. V., & Bae, H. (2015). Significance of antioxidant potential of plants and its relevance to therapeutic applications, Inter. J. Biol. Sci., vol. 11(8), pp. 982.